3D Computation of Gray Level Co-occurrence in Hyperspectral Image Cubes

Fuan Tsai, Chun-Kai Chang, Jian-Yeo Rau, Tang-Huang Lin, and Gin-Ron Liu

Center for Space and Remote Sensing Research
National Central University
300 Zhong-Da Road
Zhongli, Taoyuan 320 Taiwan
Tel.: +886-3-4227151 ext. 57619,
Fax: +886-3-4254908
ftsai@csrsr.ncu.edu.tw

Abstract. This study extended the computation of GLCM (gray level co-occurrence matrix) to a three-dimensional form. The objective was to treat hyperspectral image cubes as volumetric data sets and use the developed 3D GLCM computation algorithm to extract discriminant volumetric texture features for classification. As the kernel size of the moving box is the most important factor for the computation of GLCM-based texture descriptors, a three-dimensional semi-variance analysis algorithm was also developed to determine appropriate moving box sizes for 3D computation of GLCM from different data sets. The developed algorithms were applied to a series of classifications of two remote sensing hyperspectral image cubes and comparing their performance with conventional GLCM textural classifications. Evaluations of the classification results indicated that the developed semi-variance analysis was effective in determining the best kernel size for computing GLCM. It was also demonstrated that textures derived from 3D computation of GLCM produced better classification results than 2D textures.

1 Introduction

Texture is one of the most important features used in various computer vision and image applications. In visual interpretation as well as digital processing and analysis of remote sensing images, texture is regarded as an essential spatial characteristics and commonly used as an index for feature extraction and image classification, especially when working on high resolution airborne and satellite imagery. Computerized texture analysis focuses on structural and statistical properties of spatial patterns on digital images. These methods have been applied successfully to solve sophisticated problems, such as image segmentation [1], content-based image retrieval [2] and detecting invasive plant species [3]. Previous studies [4, 5, 6] indicated that statistics-based texture approaches are very suitable for analyzing images of natural scenes and perform well in image classification. Among the various texture computing methods, gray level co-occurrence

A.L. Yuille et al. (Eds.): EMMCVPR 2007, LNCS 4679, pp. 429–440, 2007.
© Springer-Verlag Berlin Heidelberg 2007

matrix (GLCM) originally presented by Haralick et al. [7] is probably the most commonly adopted algorithm, especially for textural feature extraction and classification of remote sensing images.

Conventional texture analysis algorithms compute texture properties in a two-dimensional (2D) image space. This may work well in panchromatic (single-band) images and multispectral imagery with limited and discrete spectral bands. However, as imaging technologies evolve, new types of image data with volumetric characteristics have emerged, for example, magnetic resonance imaging (MRI) in medical imaging and hyperspectral images in remote sensing. Directly applying traditional 2D texture analysis algorithms to these new types of imaging data will not able to fully explore three-dimensional (3D) texture features in the volumetric data sets. To address this issue, this study undertook the development of extending conventional 2D GLCM texture computation into a 3D form for better texture feature extraction and classification of hyperpectral remote sensing images.

2 Hyperspectral Volumetric Texture Analysis

Hyperspectral imaging is an emerging technology in remote sensing. With tens to hundreds of contiguous spectral bands covering visible to short-wavelength infrared spectral regions, hyperspectral remote sensing data provide rich information about ground coverage. Because of the high resolution and abundant details in the spectral domain, most existing hyperspectral analysis algorithms focused on extracting spectral features from the data sets. For example, the minimum noise fraction (MNF) transformation, spectrally segmented principal component analysis [8] and derivative spectral analysis [9,10], all aimed at extracting useful spectral features from complex hyperspectral data sets. For texture analysis of hyperspectral imagery, most researchers applied conventional 2D texture algorithms to a single band at a time and collected these 2D textures for subsequent analysis. However, with the contiguous spectral sampling, a hyperspectral data set can be considered as an image cube with volumetric characteristics as illustrated in Fig. 1. Consequently, it should be possible to treat hyperspectral imagery as volumetric data and investigate texture features in a 3D manner.

Currently, related works and applications in volumetric texture analysis are still limited. A voxel co-occurrence matrix similar to GLCM was introduced by Gao [11] to visualize and interpret 3D seismic data. A similar approach was also used in analyzing MRI data [12]. Bhalerao and Reyes-Aldasoro [13] also demonstrated a volumetric texture description for MRI based on a sub-band filtering technique similar to the Gabor decomposition [14]. Another texture description for medical imagery based on gray level run-length and class distance was proposed and achieved promising results [1, 15]. Suzuki et al. [16] also extended HLAC (higher order local autocorrelation) shape descriptors into 3D mask patterns for the classification of solid textures. These methods had one thing in common, i.e. they all dealt with isolating specific objects (body parts, organ tissues etc.) from volumetric data sets. Although they worked well in identifying target boundaries (shapes), they might not be suitable for extracting general

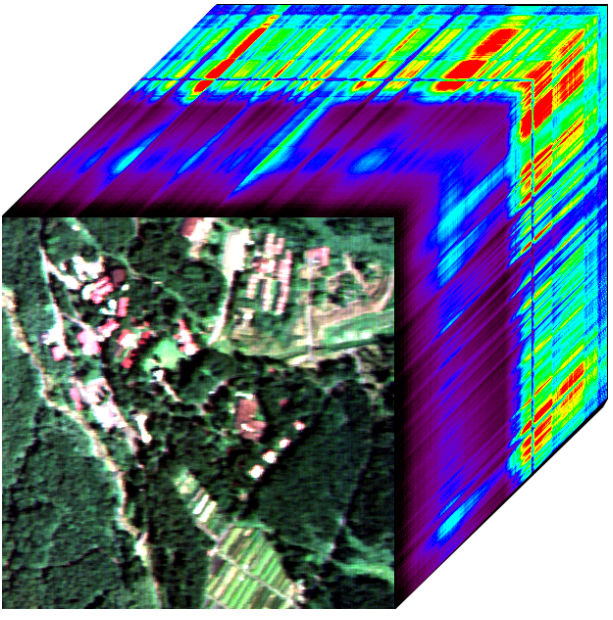

Fig. 1. Hyperspectral imagery as an image cube

texture features in hyperspectral imagery. Other types of texture description, such as models derived from Markov Random Field [17] and fractal geometry [18], might be able to extend to 3D forms, but the complexity and expense in computation could seriously limit their usability in analyzing hyperspectral image cubes. For hyperspectral remote sensing data containing natural scenes, a general gray level statistics based texture descriptor might be more appropriate and likely to achieve satisfactory feature extraction and classification results.

3 Methods and Materials

Texture features derived from GLCM are so-called second order texture calculations because they are based on the joint co-occurrence of gray values for pairs of pixels at a given distance and direction.

3.1 3D GLCM Computation

For a hyperspectral image cube with n levels of gray values, the co-occurrence matrix, M, is a n by n matrix. Values of the matrix elements within a moving box, W, at a given displacement, $d = (dx, dy, dz)$, are defined as

$$M(i,j) = \sum_{z=1}^{W_z - d_z} \sum_{x=1}^{W_x - d_x} \sum_{y=1}^{W_y - d_y} CONDITION$$
$$CONDITION = (G(x,y,z) = i \wedge G(x+d_x, y+d_y, z+d_z) = j)?1:0 \quad (1)$$

where x, y, z are denoted as the position in the moving box. In other words, the value of a 3D GLCM element, $M(i,j)$, reflects that within a moving box, how often the gray levels of two pixels, $G(x,y,z)$ and $G(x+d_x, y+d_y, z+d_z)$, with the spatial relationship of d, are equal to i and j, respectively. Theoretically, there can be numerous combinations of the spatial relationship or the displacement vector, d. However, for the simplification of computation, it is usually set as one pixel in distance and 13 combinations in horizontal and vertical directions.

The original GLCM reference [7] suggested 14 statistical measures to evaluate the properties of GLCM. However, some of them are highly correlated and only a few are recommended for use with remote sensing imagery because they are more suitable for describing features in natural scenes [19,20,21]. Four statistical measures were used in this study, including contrast (CON), entropy (ENT), homogeneity (HOM) and angular second moment (ASM) as listed from Eq. (2) to Eq. (5).

$$CON = \sum\sum \left[(i-j)^2 M_{ij} \right] \tag{2}$$

$$ENT = \sum\sum \left(M_{ij} \cdot \log M_{ij} \right) \tag{3}$$

$$HOM = \sum\sum \left\{ \frac{1}{1+(i-j)^2} M_{ij} \right\} \tag{4}$$

$$ASM = \sum\sum M_{ij}^2 \tag{5}$$

3.2 Semi-variance Analysis

Among the parameters affecting GLCM-based texture analysis, the size of the moving box (kernel) has the most significant impact. A previous study demonstrated that kernel size accounted for 90% of the variability in textural classification [22]. During the evaluation, it usually requires a large kernel size to obtain meaningful descriptions of the entire data set. However, for texture segmentation, a small moving box size is preferred in order to accurately locate boundaries between different texture regions. Therefore, it is critical to determine the most appropriate moving box size for GLCM calculations. In this regard, semi-variance analysis has been proved an effect method to find the best moving box size for GLCM computation [23, 3].

Let $Z(x_i)$ and $Z(x_i+d)$ be two pixels with a lag of d (a vector of specific direction and distance) in three dimension. For all pixel pairs in a volumetric data set, the semi-variance is defined as

$$\gamma(d) = \frac{1}{2N(d)} \sum \left[Z(x_i) - Z(x_i+d) \right]^2 \tag{6}$$

where $N(d)$ is the number of pixel pairs in the data set. A typical semi-variance curve is shown in Fig. 2. In practice, training regions of interested targets

were selected from the data set to produce variance curves of different targets. The purpose was to find the range where the semi-variance would reach its maximum (sill).

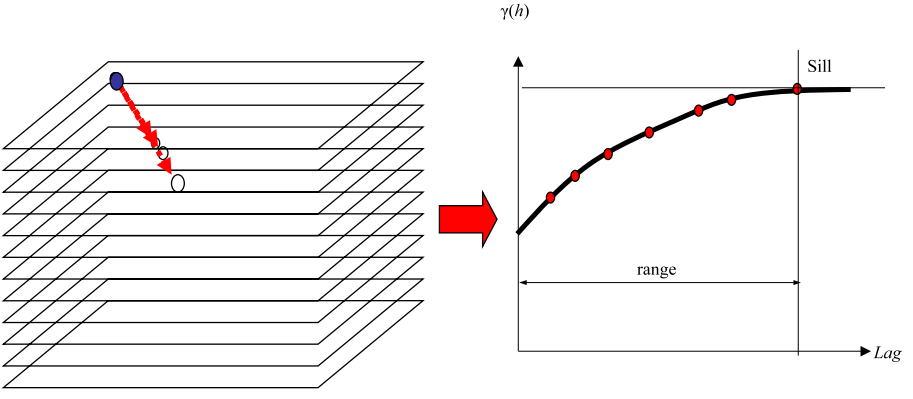

Fig. 2. Typical semi-variance curve of a 3D image cube

3.3 Test Data

Two hyperspectral data sets as displayed in Fig. 3 were used to test the performance of the developed algorithms of 3D GLCM computation and semi-variance analysis. The first data set was an EO-1 Hyperion image acquired in Jan. 2004, which covers the Heng-Chun peninsula of southern Taiwan. Hyperion is a spaceborne hyperspectral imaging spectrometer (http://eo1.usgs.gov/hyperion.php). It has 220 spectral bands covering 400-2500 nm in wavelength at a spectral sampling interval of 10 nm and a nominal 30 meter spatial resolution. Because of the low signal-to-noise ratio in the longer wavelength region, only forty five continuous bands (band-11 to band-55) in the visible to near infrared (up to the first water absorption region) were extracted from the original scene and resulting in a 481x255x45 image cube for testing.

The second image cube used was acquired with an experimental high resolution airborne hyperspectral imager called Intelligent Spectral Imaging System (ISIS) (http://www.itrc.org.tw/Publication/Newsletter/no75/p08.php) in Sep. 2006. ISIS is a pushbroom instrument with 218 spectral bands (430-945 nm at 3.5-5 nm spectral resolution). The ISIS scene has a 1.5 meter spatial resolution and covers a mountainous area with rich natural and planted forests in central Taiwan. Spectral bands (band-20 to band-210) of the same wavelength region used in the Hyperion data set were extracted from the original ISIS imagery. An 800 pixels by 800 pixels sub-image centered with nadir track was selected as the test area to minimize variations caused by the spectral "smile" effect [24] commonly seen in pushbroom sensors. Therefore, the testing ISIS data set was a 800x800x190 image cube.

(a) Hyperion (b) ISIS

Fig. 3. False color hyperspectral imagery

Other supplementary data included photo-maps, high resolution aerial photographs and landcover maps of the study areas. These data were primarily used for geo-referencing (registering) the original images, selection of training regions for semi-variance analysis and supervised classification as well as evaluating classification results.

4 Results and Discussions

Several tests were conducted on the two image cubes to evaluate performance of the developed algorithms for 3D computation of GLCM. First, a series of 3D semi-variance analysis were applied to the two image cubes. Fig. 4 shows examples of the semi-variance curves of four different targets to classify in the Hyperion data. Different colored curves in Fig. 4 represent semi-variances at different directions (azimuth, zenith) as labeled in the bottom of each plot. One thing to note in the plots of Fig. 4 is the divergency of the red curve for each target. The red semi-variance curves were computed along direction (0, 0). Unlike MRI or other solid data sets, the third (Z) axis of a hyperspectral image cube is the spectrum instead of a geometric axis. Therefore, direction (0, 0) tried to calculate variance of the same pixel at two wavelengths without any spatial consideration, thus diverging as the lag increased.

Semi-variance analysis in Fig. 4 indicated that 5 was the best kernel size for the textural analysis of the Hyperion data. To test this hypothesis, three GLCMs were generated with 3x3x3, 5x5x5 and 7x7x7 moving boxes. Supervised classifications were conducted on aforementioned four statistical measures with exactly the same training and verification data randomly selected from ground truth

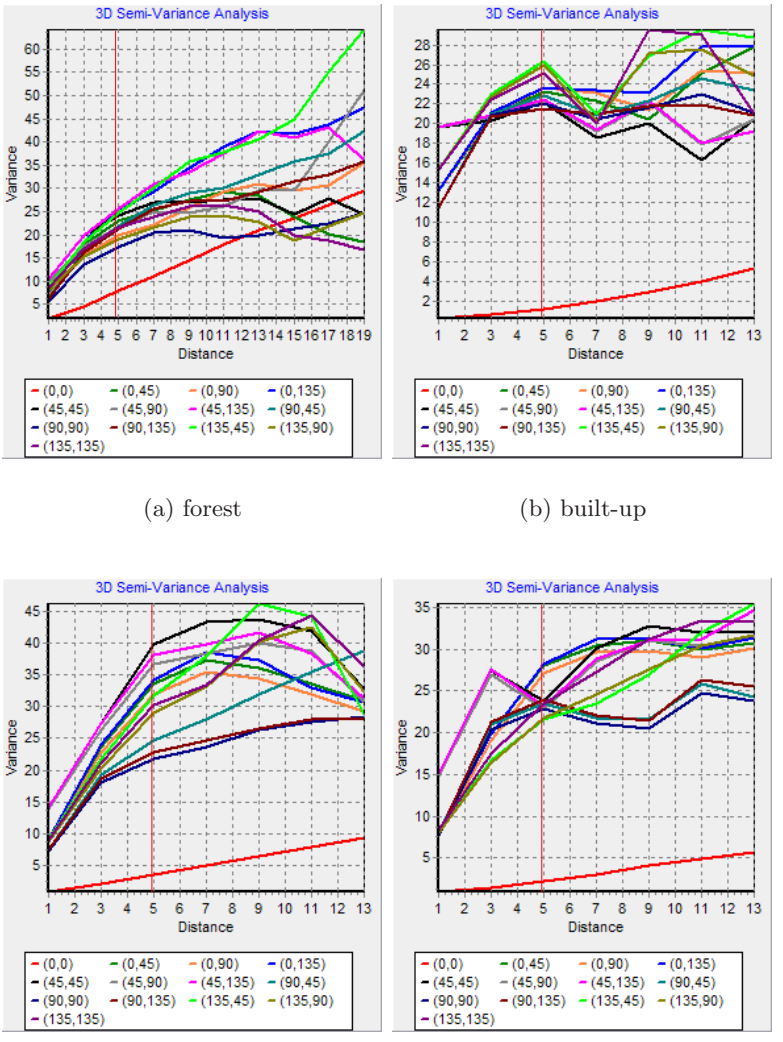

(a) forest (b) built-up

(c) grassland (d) bare ground

Fig. 4. Semivariance curves of four different targets in the Hyperion imagery

landcover maps. The overall accuracies (OA) of the classifications are plotted in Fig. 5. In this test, moving box of 5x5x5 produced the best results except the CON. This has validated the effectiveness of the developed 3D semi-variance analysis. In addition, to compare 3D GLCM computation with 2D GLCM, more thorough classifications were conducted on features extracted from five feature collections, including original spectral data, textures from 2D GLCM, textures from 3D GLCM, original plus 2D textures and original plus 3D textures with the three moving box sizes. Principal component analysis was used to select features

from the five data groups. Fig. 6 illustrates the OA and Kappa values of the classification evaluation. It is clear that 3D GLCM outperformed conventional 2D GLCM with or without the original spectral data. In addition, in the 3D GLCM cases (G2 and G4 in Fig. 6), the best results were also generated from the 5x5x5 moving box.

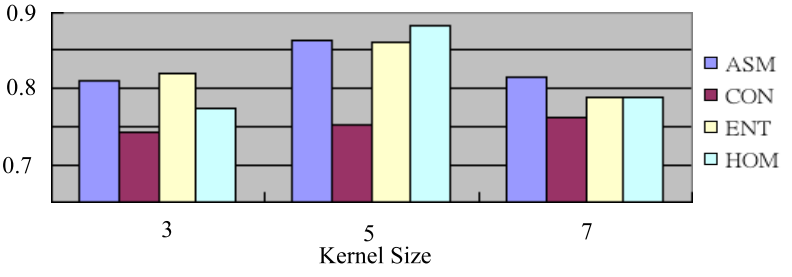

Fig. 5. Overall accuracies of different kernel sizes

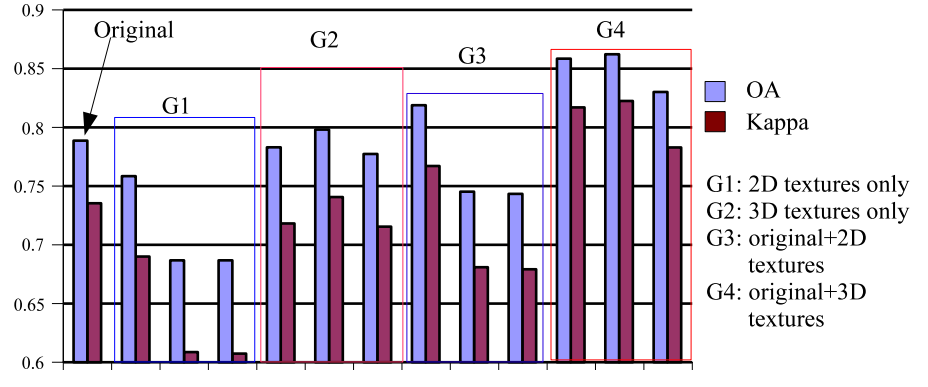

Fig. 6. Evaluations of Hyperion classifications. Each group operated on three kernel sizes (left to right: 3, 5, 7).

Similar tests were also performed on the ISIS data. There are four primary vegetation ground coverages in the ISIS scene, including Taiwania fir, Japanese cedar, maple, and bamboo. Fig. 7 displays the training regions selected for semivariance analysis and the classification results based on 2D and 3D textures calculated with a kernel size of 5. The four vegetation types are color coded as red, dark red, green and blue, respectively in Fig. 7. The training regions were selected according to landcover maps provided by a local forestry administration agency. A visual inspection on Fig. 7 reveals that 2D textural classification had completely misclassified the fir and cedar classes as maple or bamboo, while 3D textures identified most of the two classes (as well as the other two) correctly.

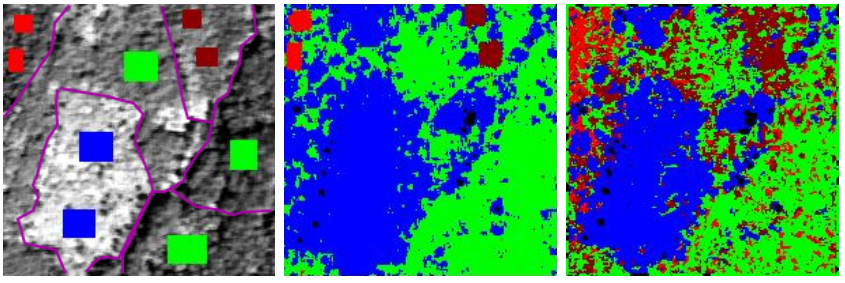

(a) training data (b) 2D GLCM (c) 3D GLCM

Fig. 7. Classification results of the ISIS data with 2D and 3D GLCM features

Semi-variance analysis on the ISIS data set suggested that 5x5x5 and 7x7x7 moving boxes were the best for 3D computation of GLCM. A series of classifications similar to the ones applied to the Hyperion data were also carried out on the ISIS data for a quantitative evaluation. The evaluation results are displayed in Fig. 8. In general, the best classification was resulted from features extracted from original spectral data plus 3D textures computed with a 7x7x7 moving box. However, it was noted that the OA differences between 3D and 2D textural classifications were insignificant. Part of the reason is because OA is an overly optimistic evaluation for classification accuracy since it does not account for omission errors. This can be contended by the observation that OA values in Fig. 8 do not reflect the high omission errors in the 2D textural classification result of Taiwania fir (red) and Japanese cedar (dark red) categories as displayed in Fig. 7. The relatively lower Kappa of 2D textural classification results is another indication of the uncertainty. Another possible reason might have to do with the characteristics of ISIS data. Because of the fine spectral resolution, texture

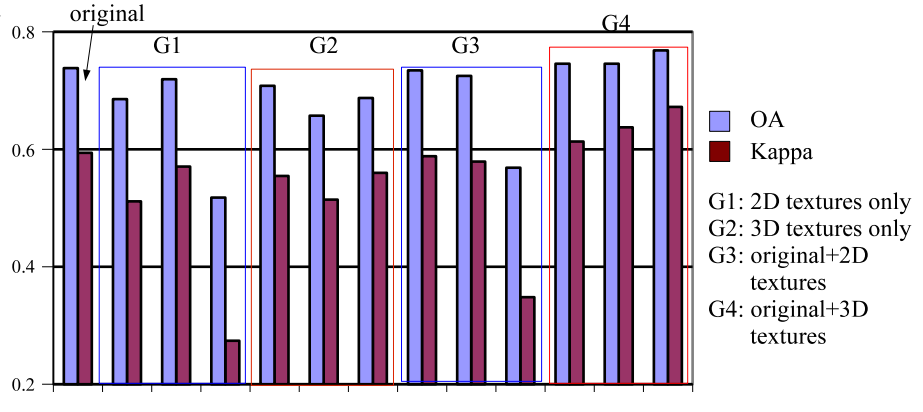

Fig. 8. Evaluations of ISIS classifications. Each group operated on three kernel sizes (left to right: 3, 5, 7).

features derived from 3D computation of GLCM may become highly correlated, thus degrading the classification performance. The impact of spectral resolution to 3D computation of GLCM in hyperspectral image cubes is still under investigation. Nonetheless, resampling the spectral resolution to a broader sampling interval (for example, from 3.5-5 nm to 10 nm as the Hyperion data) might be able to enhance the discriminability of hyperspectral 3D textures.

5 Conclusion and Future Work

This study treated hyperspectral image cubes as volumetric data sets and extended the computation of gray level co-occurrence into a 3D form to thoroughly explore volumetric texture features of hyperspectral remote sensing data. A 3D semi-variance analysis algorithm was also developed to obtain appropriate moving box (kernel) sizes for computing gray level co-occurrence in 3D image cubes. Results of tests conducted on two hyperspectral image cubes validated that the developed semi-variance algorithm was effective in determining the best moving box sizes for 3D texture description. The experiments also demonstrated that texture features derived from 3D computation of GLCM provided better classification results than features collected from conventional 2D GLCM calculations.

The results of this study suggest that 3D computation of gray level co-occurrence should be a viable approach to extract volumetric texture features from hyperspectral image cubes for classification. It is also possible to apply these techniques to other remote sensing data with volumetric characteristics, such as LiDAR data with multiple returns or electro-magnetic scans. However, there are still issues for improvement. For example, the impact of spectral resolution to the correlations of generated texture features will need to be studied in detail. Another interested research topic derived from this study will be to further develop a third-order texture descriptor to truly represent three-dimensional texture features of complicated hyperspectral and other volumetric data.

Acknowledgments

This study was supported in part by the National Science Council of Taiwan under Project No. NSC-95-2752-M-008-005-PAE. The authors would like to thank the Instrument Technology Center and the Industrial Technology Research Institute of Taiwan for kindly providing the ISIS hyperspectral imagery and other data.

References

1. Albregtsen, F., Nielsen, B., Danielsen, H.E.: Adaptive gray level run length features from class distance matrices. In: 15th International Conference on Pattern Recognition. vol. 3, pp. 3746–3749 (2000)
2. Jhanwar, N., Chaudhuri, S., Seetharaman, G., Zavidovique, B.: Content based image retrieval using motif cooccurrence matrix. Image and Vision Computing 22(12), 1211–1220 (2004)

3. Tsai, F., Chou, M.J.: Texture augmented analysis of high resolution satellite imagery in detecting invasive plant species. Journal of the Chinese Institute of Engineers 29(4), 581–592 (2006)
4. du Buf, J.M.H., Kardan, M., Spann, M.: Texture feature performance for image segmentation. Pattern Recognition 23(4), 291–309 (1990)
5. Ohanian, P.P., Dubes, R.C.: Performance evaluation of four classes of texture features. Pattern Recognition 25(8), 819–833 (1992)
6. Reed, T.R., du Buf, J.M.H.: A review of recent texture segmentation and feature extraction techniques. CVGIP: Image Understanding 57(3), 359–372 (1993)
7. Haralick, R.M., Shanmugan, K., Dinstein, I.: Texture features for image classification. IEEE Trans. Systems, Man Cybernetics 3(6), 610–621 (1973)
8. Tsai, F., Lin, E.K., Yoshino, K.: Spectrally segmented principal component analysis of hyperspectral imagery for mapping invasive plant species. International Journal of Remote Sensing 28(5-6), 1023–1039 (2007)
9. Tsai, F., Philpot, W.: A derivative-aided image analysis system for land-cover classification. IEEE Transactions on Geoscience and Remote Sensing 40(2), 416–425 (2002)
10. Tsai, F., Philpot, W.D.: Derivative analysis of hyperspectral data. Remote Sensing of Environment 66(1), 41–51 (1998)
11. Gao, D.: Volume texture extraction for 3D seismic visualization and interpretation. Geophsics 68(4), 1294–1302 (2003)
12. Mahmoud-Ghoneim, D., Toussaint, D., Constans, J.M., de Certaines, J.D.: Three dimensional texture analysis in MRI: a preliminary evaluation in glioma. Magnetic Resonance Imaging 21(9), 983–987 (2003)
13. Bhalerao, A., Reyes-Aldasoro, C.C.: Volumetric texture description and discriminant feature selection for MRI. In: Moreno-Díaz Jr., R., Pichler, F. (eds.) EUROCAST 2003. LNCS, vol. 2809, pp. 573–584. Springer, Heidelberg (2003)
14. Unser, M.: Texture classification and segmentation uisng wavelet frames. IEEE Trans. on Image Processing 4(11), 1549–1560 (1995)
15. Nielsen, B., Albregtsen, F., Danielsen, H.E.: Low dimensional adaptive texture feature vectors from class distance and class difference matrices. IEEE Trans. Medical Imaging 23(1), 73–84 (2004)
16. Suzuki, M.T., Yoshino, Y., Osawa, N., Sugimoto, Y.Y.: Classification of solid texture using 3D mask patterns. In: 2004 IEEE International Conference on Systems, Man and Cybernetics, pp. 6342–6347 (2004)
17. Cross, G.R., Jain, A.K.: Markov Random Field texture models. IEEE Trans. on PAMI 5(1), 25–39 (1983)
18. Keller, J.M., Chen, S.: Texture description and segmentation through fractal geometry. Computer Vision, Graphics and Image Processing 45, 150–160 (1989)
19. Baraldi, A., Parmiggiani, F.: An investigation of the textural characteristics associated with gray level cooccurrence matrix statistical parameters. IEEE Transactions on Geoscience and Remote Sensing 33, 293–303 (1995)
20. Clausi, D.A.: An analysis of co-occurrence statistics as a function of grey level quantization. Canadian J. Remote Sensing 28, 45–62 (2002)
21. Jobanputra, R., Clausi, D.A.: Preserving boundaries for image texture segmentation using grey level co-occurring probabilities. Pattern Recognition 39, 234–245 (2006)

22. de Martino, M., Causa, F., Serpico, S.B.: Classification of optical high resolution images in urban environment using spectral and textural information. In: IEEE International Geoscience and Remote Sensing Symposium (IGARSS'03). vol. 1, pp. 467–469 (2003)
23. Kourgli, A., Belhadj-Aissa, A.: Texture primitives description and segmentation using variography and mathematical morphology. In: IEEE International Conference on Systems, Man and Cybernetics. vol. 7, pp. 6360–6365 (2004)
24. Datt, B., McVicar, T.R., van Niel, T.G., Jupp, D.L.B., Pearlman, J.S.: Preprocessing EO-1 Hyperion hyperspectral data to support the application of agricultural indexes. IEEE Transactions on Geoscience and Remote Sensing 41, 1246–1259 (2003)